



Research article

## Application of Agrowaste-based Hydrochar as Soil Amendments and Its Utilization for Lead Adsorption

Imran Chowdhury Sakib<sup>1</sup>, Md. Azharul Islam<sup>2\*</sup>, Rashedul Islam<sup>1</sup>, Jeba Rezwana<sup>1</sup> and Md. Atikul Islam<sup>1\*</sup>

<sup>1</sup>*Environmental Science Discipline, Khulna University, Khulna-9208, Bangladesh*

<sup>2</sup>*Forestry and Wood Technology Discipline, Khulna University, Khulna-9208, Bangladesh*

### ABSTRACT

Lead (Pb) contamination in Bangladesh requires cost-effective and sustainable remediation solutions to protect the population from devastating health consequences. This study attempted to develop a convenient method to reduce the amount Pb from soil. Chicken feather hydrochar (CFH) was prepared by hydrothermal carbonization (HTC) at 160 °C for 3 h. Subsequently, a CFH-soil mixture was used for Pb adsorption via several batch adsorption experimental parameters; initial concentration, temperature, contact time, and pH. The study investigated the adsorption equilibrium, isotherms, kinetics, as well as the thermodynamics, specifically analyzing the impact of the initial pH on the removal process. The findings revealed that the Langmuir model provided a more accurate explanation of the adsorption process than the Freundlich model. The highest limits of adsorption capacities were 671.1, 1426, and 1044 mg/g at 30, 40, and 50 °C respectively, according to Langmuir model. The study also showed that there was an increase of adsorption capacity (233 mg/g) up to pH 4 and then gradually decreased. This may be due to the pH point of zero charge ( $pH_{pzc}$ ) of 4.5. The most accurate depiction of the kinetic data was provided by the pseudo-second-order kinetic model. In a thermodynamic analysis, it was determined that adsorption is a spontaneous, practical, endothermic process that has a strong affinity for Pb. The study highlights CFH as a promising solution for mitigating Pb contamination in soil. Additional micro-level field trials are necessary to evaluate the CFH's effectiveness in practical applications.

### Introduction

Lead (Pb) is a toxic heavy metal that damages organs and systems including nervous systems (Gilani et al., 2015), kidney (Assi et al., 2016), heart (Flora et al., 2012), and bone (Debnath et al., 2019). Due to the actions carried out by humans, Pb, a naturally occurring element, is subjected to environmental modifications. There are many scholarly investigations that have been done to examine the possible associations between Pb and a wide range of health disorders. Santurtún et al. (2016) and Nigg et al. (2008) investigated the correlation between motor neuron disease and Pb. In a similar vein, research carried out by Gorini et al. (2014), Rossignol et al. (2014), and Kennedy et al. (2012), respectively, examined correlations with autism and preeclampsia. While Navas-Acien et al. (2007) looked into the Pb bioaccumulation effect on cardiac disease, Earl et al. (2016) concentrated on developmental deficits in children. The possible link between Pb bioaccumulation

and attention deficit hyperactivity disorder (ADHD) was examined by Goodlad et al. (2013).

The connection between Pb and mental illness was further clarified by Guilarte et al. (2012), while Wu et al. (2012) investigated possible connections to brain cancer. Taken as a whole, these studies offer insightful information about the complex interactions between Pb and many health issues. It has been discovered that elevated Pb levels in kids are associated with decreased IQ, impaired cognitive function, and behavioral issues (Nigg et al., 2008; Nevin, 2000). Pb pollution from industrial and non-industrial sources has received increasing attention in recent years, mainly because of growing concerns about public health (Schroeder, 1965). Due to the burning of leaded gasoline by cars, there has been a discernible rise in Pb concentrations in plants and in the soil near roadways (Cannon & Bowles, 1962; Motto et al., 1970). Moreover, it has been noted that the Pb concentration of street dust

### ARTICLE INFO

#### **Article timeline:**

Date of Submission:

24 February, 2024

Date of Acceptance:

16 June, 2025

Article available online:

26 June, 2025

#### **Keywords:**

Hydrothermal carbonization

Chicken feather

Hydrochar

Lead

Adsorption

Soil

\*Corresponding authors: [atik@es.ku.a.bd](mailto:atik@es.ku.a.bd)

has increased as well (Archer & Barratt, 1976; Day et al., 1975). A previous study found that Pb levels are significantly higher in the soil, crops, water, air, and vegetables near Bangladesh's cities and industrial areas (Islam et al., 2015). Two and three-stroke engines have contributed to Bangladesh's atmospheric Pb pollution during the 20th century (Begum et al., 2014). In Bangladesh, 148 informal recycling sites process used lead acid batteries (ULAB) and 97 lead acid battery manufacturing plants. Geostatistical surveys have revealed that the concentrations of Pb in soil exhibit a wide range, spanning from a mean value of 21.4 ppm to as high as 3467 ppm (Markus & McBratney, 2001).

Adsorption has emerged as an exceedingly convenient and efficacious method for attaining optimal effectiveness in the elimination of heavy metals (HM) when juxtaposed with alternative conventional methodologies. The inherent nature of all adsorbents necessitates the presence of functional groups that serve a pivotal function in the adsorption of metal ions. The scholarly work conducted by Chakraborty et al. (2022) is of notable significance. The utilization of adsorbents derived from economically viable biomass residuals has garnered considerable interest within the scholarly scientific community owing to their remarkable efficacy in the remediation of environmental pollution (Kambo & Dutta, 2015). One of the prominent examples of the adsorbent material is hydrochar, which is under consideration.

Hydrothermal carbonization (HTC) can be referred to as a thermochemical procedure that is considered for its noteworthy energy efficiency (Mau et al., 2016). This method fosters the transformation of biomass into a solid substance, known as hydrochar, which bears a resemblance to coal. Notably, this conversion takes place under conditions that are fairly favorable (Xu et al., 2013). Hydrochar, a material that garnered significant attention, has the potential to serve as a precursor for activated carbon that can be employed in soil remediation works (Wang et al., 2018). Moreover, hydrochar is proven to be effective in the adsorption of HMs, according to the study of Mihajlović et al. (2016) and Xue et al. (2012). According to the investigation undertaken by Hammud et al. (2021), adsorption using hydrochar exhibits a higher degree of efficacy in the removal of Pb in comparison with the utilization of biochar.

As a by-product, the poultry business generates chicken feathers (CFs), amounting to about 10% of the chicken's weight. According to literature, a noteworthy amount, millions of metric tons, of CFs are being produced annually in Bangladesh. It is a matter of misfortune that this garbage is haphazardly dumped into the environment without performing any sort of industrial treatment to reduce the damaging effects of that garbage, as concluded by Akter et al. (2019). The main component of feathers, making up over 90% of their total mass (Grazziotin et al., 2006), is keratin, an incredibly inconvenient and vexing byproduct (Wrzeniewska-Tosik & Adamiec, 2007). The avian waste, CF, can be effectively utilized by converting them into hydrochar with the help of the HTC technique. CFs, which consist of biomasses abundant in keratin, exhibit a notable lack of biodegradability. However, a promising solution to mitigate environmental pollution

and waste associated with CFs lies in their conversion into hydrochar.

Therefore, this study aimed at investigating the utilization of cost-effective and easily available materials that do not necessitate intricate modification procedures for their potential application in the removal of Pb. Furthermore, the altered agrowaste has the potential to be utilized as soil amendments. Therefore, the primary aims of the investigation were the following: (1) to ascertain the prospective efficacy of CFH in the elimination of Pb and (2) to establish the kinetics, thermodynamics, and adsorption mechanism governing the interaction between Pb and CFH mixed soil.

## Materials and Methods

### Soil preparation

Systematic collection of soil samples was conducted at different geographical coordinates within the renowned premises of Khulna University, located in the city of Khulna, Bangladesh. The aforementioned soils were extracted from the uppermost stratum, specifically the surface layer spanning a depth of 0 to 20 cm. Subsequently, the soils underwent a process of desiccation over a span of seven days, wherein they were exposed to the surrounding atmospheric conditions in order to diminish their moisture content. The subsequent procedure entailed exerting pressure upon the soil, subsequently followed by the act of sieving through a mesh with a fineness of 2 mm, thereby facilitating subsequent analysis.

### Preparation of CFH

The CFs gathered from the local market (Gollamari Bazar) were subjected to a cleaning process using water, followed by air drying at ambient temperature. Subsequently, the desiccated feathers were grinded and stored in a tightly sealed container in advance of the experiment. Hydrochar production involved subjecting the CFs to HTC within a 300-mL reactor. Specifically, 7 g of ground CFs were introduced into the reactor, along with distilled water (100 mL), ensuring complete submersion. The HTC process was conducted under controlled internal pressure for a duration of 1-3 hours, within a temperature range of 150-170 °C. In order to get the maximum yield percentage of hydrochar, the Box-Behnken approach was utilized to construct a surface response model and desirability function. The optimal parameters for achieving a high hydrochar yield percentage were determined to be a temperature of 150 °C and residence times of 1 hour. The observed maximum yield percentage was approximately 51.93%. The conditions that were optimized in a certain manner, as previously indicated (Islam et al., 2021). In accordance with the HTC procedure, the reactor was subjected to cooling until it reached the surrounding temperature. Subsequently, the suspension underwent filtration to isolate the solid carbonaceous products. These products were then subjected to oven-drying for a duration of 24 hours at a temperature of 70 °C.

### Preparation of Pb solution and determination of analytical concentration

By dissolving an appropriate quantity of lead (II) nitrate ( $\text{Pb}(\text{NO}_3)_2$ ) in a 0.01 M calcium chloride ( $\text{CaCl}_2$ ) solution, a solution containing 1000 ppm of Pb was created. By

diluting the initial stock solution, the appropriate concentrations (100, 250, 500, 750, and 1000 ppm) were attained. 0.05 M HCl and 0.05 M NaOH solutions were used to modify the pH (Chakraborty et al., 2022).

### Experiments on batch adsorption

For each test, batch adsorption experiments were conducted in 250 mL cylinder flasks containing 10 g of the soil-char mixture. Temperatures of 30, 40, and 50 °C were utilized. Using a water bath shaker (GEMMYCO), 250 mL of Pb solution was combined with a 1% w/w adsorbent with a pH range of 1 to 12. The solution was introduced at concentrations of 100, 250, 500, 750, and 1000 ppm. To control the initial solution's pH, incremental adjustments were made using either 0.05 M HCl or 0.05 M NaOH. The pH measurements were determined using a pH meter (Systronics Digital pH Meter-802). The soil-char solutions were shaken (120 rpm) for 24 hours at the directed temperature. After adsorption, the resulting solutions were promptly subjected to filtration utilizing filter paper (Whatman no. 42) in order to retrieve the adsorbent. Subsequently, the supernatant solutions underwent analysis employing an atomic adsorption spectrophotometer (AA 6200, Shimadzu, Japan).

### Removal percentage estimation

After gathering all the data, the percentage removal (%removal) and adsorbed amounts were calculated. The %removal of the CFH was determined by the absorbance of the Pb. The quantification of Pb uptake by CFH was established through the deviation in Pb's bioavailable concentration from the starting concentration.

The equation for removal percentage can be expressed as following:

$$\% \text{Removal} = \frac{C_0 - C_e}{C_0} \times 100 \quad (1)$$

The initial Pb concentration,  $C_0$ , is expressed in mg/L in this equation, whereas the equilibrium Pb concentration,  $C_e$ , is also expressed in mg/L.

Furthermore, the equation pertaining to the quantification of adsorbed quantities can be elegantly formulated in the following manner:

$$\text{Amounts adsorbed, } q_e = \frac{(C_0 - C_e) V}{W} \quad (2)$$

The variable  $q_e$  represents the equilibrium adsorbed quantities of Pb on CFH, measured in mg/g.  $W$  denotes the mass of CFH in g, whereas  $V$  represents the volume of the Pb solution in L.

## Results and Discussion

### Characterization of soil and CFH

Soil properties are displayed in Table 1. The soil texture was sand 24.50%, silt 35%, clay 40.50% which indicates clay soil according to the soil texture calculator developed by the United States Department of Agriculture (USDA) similar to the result of Adhikari et al. (2006). The pH of soil was 7.63 which indicates very slightly alkaline soil. The soil exhibited an electric conductivity (EC) value of 736  $\mu\text{S/cm}$ . The pH and EC values are comparable to those reported by Joardar & Halder (2013). It was estimated that the soil has a cation exchange capacity (CEC) of about 2.30  $\text{cmol kg}^{-1}$ . The organic carbon of the soil was 31.47%. In metal recycling, soil organic carbon plays a vital role (Qishlaqi et al., 2008). The soil had a total of 0.09  $\text{mg kg}^{-1}$  of Pb. However, the bioavailability of Pb was 0  $\text{mg kg}^{-1}$ . The findings of Pb value can be justified by literature Joardar & Halder (2013). Phosphorus count was about 66.8% that is within the range (Ministry of Agriculture, 2018).

The analysis of Table 2 reveals that the hydrochar sample conveyed a carbon content of 57.41%. Nitrogen and phosphorus content are of 140.2 g/kg and 0.43 g/kg, respectively. The amount of Fe, Al, and Mn were 0.64, 1.41 and 0.37 mg/g, gradually. The characteristics of the hydrochar are identical to those reported by Akter et al. (2021). The pH of the CFH was measured to be 5.5. The higher carbon content, compared to raw chicken feathers, may contribute to maintaining good soil health, which is essential for plant growth (Anderson, 2018; Holatko et al., 2022; Islam et al., 2021). Both nitrogen and phosphorus are essential for plant growth, although their required quantities vary (Hue & Silva, 2000). The byproduct of HTC is usually acidic like we found (Kalderis et al., 2014).

Table 1: Selected properties of the experimental soil

Parameter	Amount	Unit
pH	7.63	-
EC	736	$\mu\text{S/cm}$
CEC	2.30	$\text{cmol kg}^{-1}$
Total carbon	18.25	%
Organic carbon	31.47	%
Sand	24.50	%
Silt	35	%
Clay	40.50	%
Total lead	0.09	$\text{mg kg}^{-1}$
Available lead	0	$\text{mg kg}^{-1}$
Total phosphorus	66.8	$\text{mg kg}^{-1}$

Table 2: Characteristics of chicken feather hydrochar (CFH)

Parameter	Unit	Hydrochar
Carbon	%	57.41
Nitrogen	g/kg	140.2
Phosphate	g/kg	0.43
Iron	mg/g	0.64
Al	mg/g	1.41
Mn	mg/g	0.37
pH		5.5

### Effects of pH on Pb adsorption

An investigation was conducted to examine the influence of solution pH on the absorption of Pb onto CFH, covering a pH range of 2 to 12. According to the data presented in Fig. 1, there was an initial increase followed by a subsequent drop in the quantity of Pb absorbed by CFH as the solution pH increased. The adsorbed amount at the initial pH was recorded as 222.3 mg/g. Although both  $\text{Pb}^{2+}$  and  $\text{H}^+$  ions compete to bond with the adsorbent, the adsorption of  $\text{H}^+$  ions is favored over  $\text{Pb}^{2+}$  at a lower pH level (Malool et al., 2021). The adsorption of Pb increases when  $\text{Pb}^{2+}$  ions replace  $\text{H}^+$  ions due to the deprotonation of functional groups at higher pH levels (Wang et al., 2018). Subsequently, it exhibited a progressive increase until reaching a maximum value of 233 mg/g at pH 4. Most of the studies have found the maximum adsorption at similar pH (Malool et al., 2021; Xia et al., 2019). However, beyond this point, the adsorbed amount started to drop, ultimately reaching a minimum value of 1.3 mg/g at pH 12.

The pH point of zero charge ( $\text{pH}_{\text{pzc}}$ ) indicates a certain level of pH where the surface charge of an adsorbent stays in a neutral state. It provides important information about the potential electrostatic interaction mechanism the adsorbent and the adsorbate (Islam et al. 2021). The  $\text{pH}_{\text{pzc}}$  of CFH was calculated to be 4.5. The surface of the CFH will show positive charge below the  $\text{pH}_{\text{pzc}}$ . Conversely, at a pH more the  $\text{pH}_{\text{pzc}}$ , the CFH surface will be negatively charged. When pH increased from 2 to higher, the rate of dissociation also increased. Consequently, the number of negative ions increased in the solution resulting increased Pb adsorption because of the electrostatic attraction. Above  $\text{pH}_{\text{pzc}}$ , the Pb adsorption decreased quickly due to the electrostatic repulsion between the negatively charged surface of the CFH and Pb ion. Moreover, the highest adsorption capacity was found at pH 4 which supported the concept of  $\text{pH}_{\text{pzc}}$ . Madduri et al. (2020) also found similar result to this study.

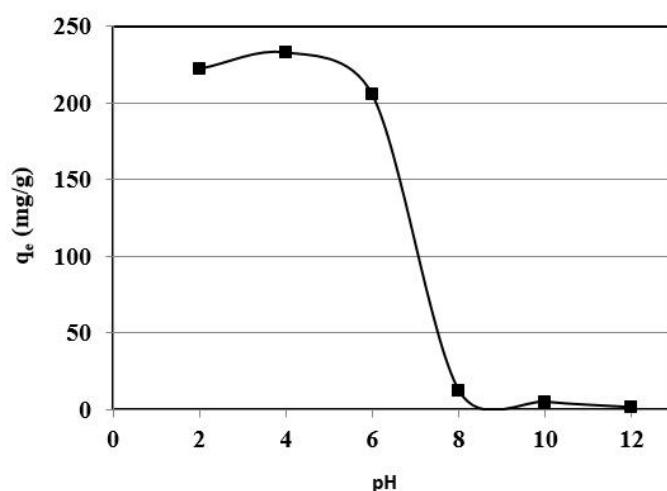


Figure 1: Effect of solution pH on Pb adsorption at 30 °C (Pb initial concentration, 500 mg/L; agitation speed, 120 rpm; CFH dose, 0.1 mg)

### Adsorption isotherms of Pb on CFH

Adsorption isotherm provides insights about the equilibrium condition of Pb distribution between the solid and liquid phases. Nonlinear Langmuir and Freundlich models were employed to interpretate the isotherm equilibrium data. The interpretation offers a comprehensive evaluation of the behavior that the Pb molecules show in relation to CFH.

The Langmuir isotherm model is applied to describe the situation where the adsorbent surface exhibits

homogeneity, and solutes are primarily confined to specific surface sites. Moreover, it suggests that the solutes do not diffuse into other layers of particles and the mechanism is compatible with monolayer adsorption. The Langmuir equation, proposed by Langmuir (1918), is expressed in a non-linear form as follows:

$$q_e = \frac{q_m K_a C_e}{1 + K_a C_e} \quad (3)$$

In this context, the parameters involved include  $q_e$ , representing the adsorbed amount at equilibrium in mg/g, and  $C_e$ , indicating the equilibrium concentration in mg/L. The Langmuir constants, denoted as  $q_m$  (mg/g) and  $K_a$  (L/mg), are associated with the adsorption capacity and adsorption rate, respectively.

The Freundlich isotherm provides mathematical equation that characterize sorption on surfaces exhibiting heterogeneity and distribution of non-uniform energy. The mathematical expression for it is as follows:

$$q_e = K_F C_e^{1/n} \quad (4)$$

Here,  $q_e$  denotes the adsorbed amount measured in mg/g. The equilibrium concentration ( $C_e$ ) expressed in mg/L. The Freundlich coefficient, denoted as  $K_F$ , performs as a measure of the extent or intensity of adsorption. Additionally,  $1/n$  represents a coefficient of exponential that provides insights into the curvature and energy distribution within the isotherm. A larger value of  $1/n$  indicates a stronger attraction between the substance being adsorbed and the variations in the sites of the adsorbent.

The selection of the ideal isotherm model is based on evaluating the correlation coefficient ( $R^2$ ) value and further supported by validating it using a non-linear error metric, namely the residual root-mean squared error (RMSE). The evaluation involves the application of the subsequent formulas:

$$R^2 = 1 - \frac{\sum_{N=1}^N (q_{e.exp.N} - q_{e.mod.N})^2}{\sum_{N=1}^N (q_{e.exp.N} - \bar{q}_{e.exp.N})^2} \quad (5)$$

$$RMSE = \sqrt{\frac{1}{N-1} \sum_{N=1}^N (q_{e.exp.N} - q_{e.mod.N})^2} \quad (6)$$

Here,  $q_{e.exp}$  is the experimental adsorption capacities at equilibrium in mg/g. While  $q_{e.mod}$  expresses the isotherm model-predicted adsorption capacities at equilibrium in mg/g. And,  $N$  denotes the total observation numbers in the study.

Table 3 displays the isotherm characteristics, which include the Freundlich and Langmuir isotherm parameters, for the Pb adsorption onto CFH at different temperatures. The observed adsorption capacities ( $q_m$ ) obtained from the application of the adsorption isotherm model, specifically the Langmuir model, displayed an ascending pattern when the temperature was elevated from 30 to 40 °C. However, subsequent increments in temperature from 40 to 50 °C resulted in a subsequent decrease in the adsorption capacities. This occurrence demonstrated that the reaction of adsorption exhibited an initial endothermic nature at 40 °C, followed by a subsequent exothermic nature at 50 °C. Nevertheless, it is worth noting that the augmentation of temperature from 30 to 40 °C, followed by further increments, resulted in a discernible decline in the adsorption capacities as depicted in the Freundlich isotherm models (Table 3), specifically denoted as  $K_F$ . The Langmuir isotherm model consistently yielded higher  $R^2$  values across the three examined temperatures, as detailed in Table 3. Moreover, the Langmuir model demonstrated lower RMSE values when compared to the Freundlich isotherm model. The obtained result implies that the process of Pb adsorption on CFH was more accurately characterized by the Langmuir model. In another investigation, it was observed that the Langmuir model isotherm exhibited the most suitable fit for the experimental data related to Pb adsorption on activated hydrochar derived from palm leaves, as reported by Hammud et al. (2021).

Figure 2 (a-c) demonstrates the observed point of the adsorbed amount ( $q_e$ ) against the equilibrium concentration ( $C_e$ ) at 30, 40 and 50 °C respectively.

Table 3: Langmuir and Freundlich isotherm parameters for the adsorption of Pb onto CFH at different temperatures

Temperature (°C)	Langmuir					Freundlich				
	$q_m$	$K_a$	$R^2$	RMSE	$\chi^2$	$K_F$	$n$	$R^2$	RMSE	$\chi^2$
30	671.1	0.012	0.999	7.501	330.004	73.36	0.598	0.993	9.821	332.79
40	1426	0.003	0.999	5.857	630.12	21.758	0.581	0.933	37.52	649.69
50	1044	0.008	0.999	12.928	836.671	42.20	0.507	0.998	5.66	597.34

### Adsorption thermodynamics

The analysis of thermodynamic parameters associated with the adsorption phenomenon, encompassing the standard free enthalpy change ( $\Delta H^\circ$ ), energy change ( $\Delta G^\circ$ ), and entropy change ( $\Delta S^\circ$ ), assumes a pivotal role in ascertaining the thermodynamic viability and inherent spontaneity of the process of adsorption. Calculations of these parameters are conducted using the Van't Hoff formula:

$$\ln K_p = \frac{\Delta S^\circ}{R} - \frac{\Delta H^\circ}{RT} \quad (7)$$

In this formula,  $K_p$  represents the adsorption distribution coefficient. The universal gas constant,  $R = 8.314$  J/mol K whereas the absolute temperature ( $T$ ) represented in Kelvin. This expression was used to determine the value of  $K_p$ , which is as follows:

$$K_p = \frac{C_e^{ads}}{C_e^{sol}} \quad (8)$$

The notation  $C_e^{ads}$  represents the state of equilibrium wherein the concentration of Pb on the adsorbent is quantified in mg/L. And  $C_e^{sol}$  denotes the equilibrium concentration of Pb in the solution, also measured in mg/L. The determination of  $\Delta H^\circ$  (enthalpy change) and  $\Delta S^\circ$  (entropy change) involved the estimation of these values from the slope and intercept, respectively, of the linear Van't Hoff representation of  $\ln K_p$  versus  $1/T$ .

In order to determine the  $\Delta G^\circ$ , the equation that is used is as follows:

$$\Delta G^\circ = \Delta H^\circ - \Delta S^\circ T \quad (9)$$

Equilibrium experiments were conducted at temperatures of 30, 40, and 50 °C to assess the efficacy of Pb adsorption by CFH. Table 4 presents the thermodynamic parameters that were determined at various temperatures, particularly  $\Delta H^\circ$ ,  $\Delta G^\circ$ , and  $\Delta S^\circ$ . The negative  $\Delta G^\circ$  values observed at all temperatures indicate that the process of Pb adsorption onto CFH is a feasible and spontaneous method, accompanied by a substantial

release of energy. Furthermore, a decrease in  $\Delta G^\circ$  values with rising temperature suggests that the adsorption of Pb onto CFH is thermodynamically favorable, particularly at elevated temperatures.

The positive value of  $\Delta H^\circ$  (10.686 kJ/mol) at the investigated temperature intervals of 30, 40, and 50 °C elucidates the endothermic nature of adsorption, specifically pertaining to the chemisorption mechanism. However, it is important to note that this particular phenomenon does not meet the established criteria outlined in the definition of chemisorption. As per the research findings of Faust and Aly (1987), it is suggested that chemisorption enthalpy alterations below the threshold of 84 kJ/mol are to be classified as manifestations of physical adsorption. Henceforth, it can be concluded that in this particular investigation, the

process of Pb adsorption onto the CFH material was predominantly attributed to physisorption. The observed  $\Delta S^\circ$  value (0.087 kJ/mol/K) implies that the adsorption process is characterized by increased randomness (Thamer et al., 2019). This suggests that CFH has a favourable affinity for Pb (Salman et al., 2011). This occurrence is a prevalent outcome of physical adsorption, which can happen through electrostatic interactions. A comparable pattern in the values of  $\Delta H^\circ$ ,  $\Delta G^\circ$ , and  $\Delta S^\circ$  for Pb adsorption has been observed in other studies (Ali et al., 2019; Koprivica et al., 2023; Li et al., 2020).

Table 5 presents a comparative analysis of the adsorption capacity of several adsorbents utilized for the Pb removal. The data presented in Table 5 indicates that CFH is an exceptional adsorbent for eliminating Pb because of its outstanding surface structures.

Table 4: Thermodynamic parameters for the adsorption of pb onto CFH-soil mixture

$\Delta G^\circ(\text{kJ mol}^{-1})$		$\Delta H^\circ(\text{kJ mol}^{-1})$	$\Delta S^\circ(\text{kJ mol}^{-1}\text{K}^{-1})$
303.15K	-15.524	10.686	0.087
313.15K	-16.597		
323.15K	-17.249		

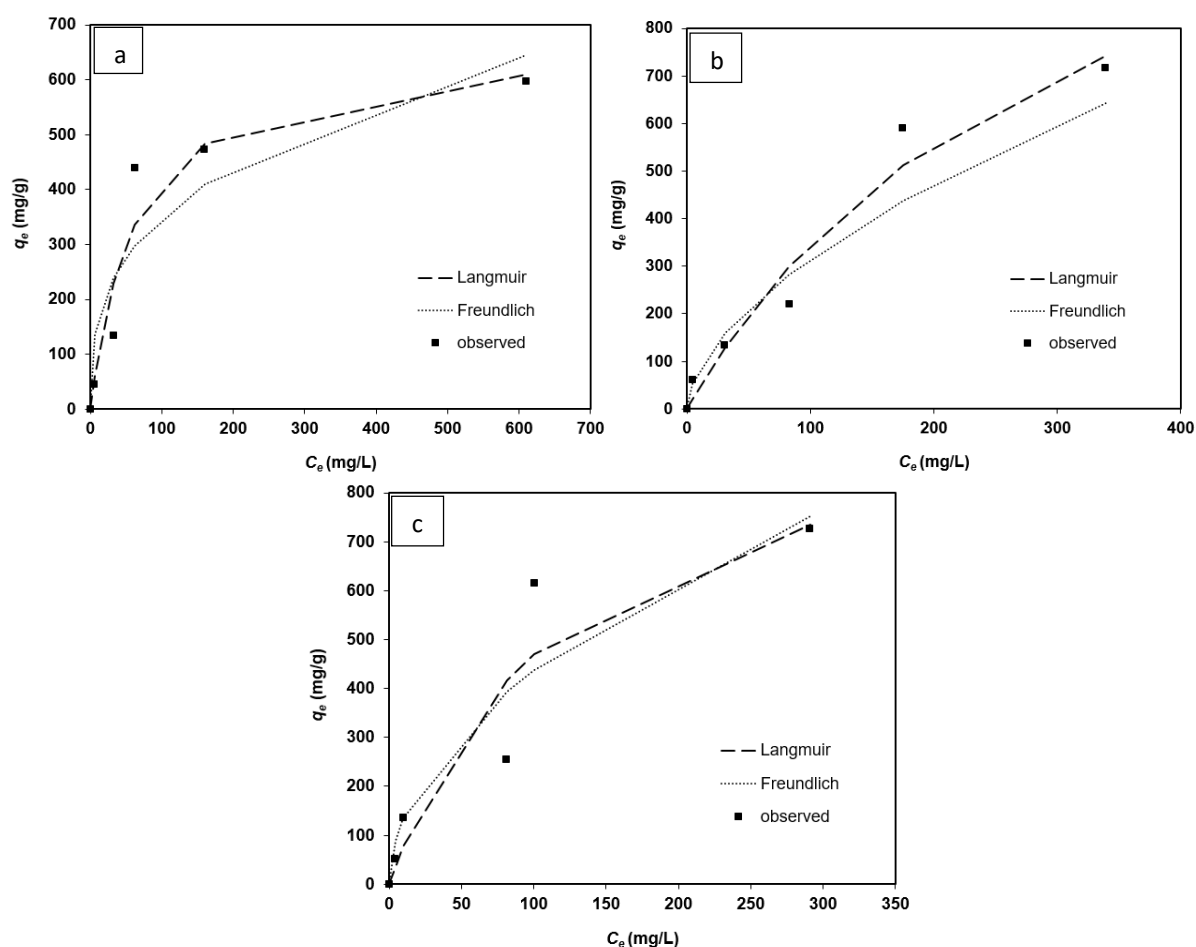


Figure 2: Adsorption isotherm fitting for adsorption of Pb onto CFH at 30 (a), 40 (b) and 50 °C (c)

Table 5: Adsorption capacity of different adsorbents

Adsorbents	Concentration (mg/L)	Adsorption capacity (mg/g)	References
CFH	0-1000	1426	This study
Bamboo hydrochar		153.85	(Hu et al., 2022)
Fresh banana peels hydrochar	300	237.90	(Ge et al., 2022)
Canola straw biochar	0-200	165	(Nzediegwu et al., 2021)
Dithiocarbamate-modified hydrochar	25-400	151.51	(Li et al., 2020)
Modified hydrochar of sawdust		92.80	(Xia et al., 2019)

### Effect of initial concentration and contact time

In any adsorption experiment, the equilibrium contact time is of utmost significance when it comes to calculate the adsorption capacity of the particular adsorbent. Figure 3 illustrates the correlation between the initial concentration and contact time in relation to the removal of Pb by CFH. The inquiry into the phenomenon of adsorption was conducted utilizing a diverse range of predetermined durations of contact and initial concentrations. For the purpose of this investigation, six different initial concentrations of Pb were chosen: 0, 100, 250, 500, 750, and 1000 mg/L. The adsorbent dosage was kept constant at 30 °C. It has been ascertained that the absorption of Pb exhibited notable velocity during the initial phase, yet progressively decreased until attaining a state of equilibrium (Paranavithana et al., 2016). After the equilibrium time of 8 h, there was no significant adsorption that was observed. Prior research (Islam et al., 2021) has documented that the CFH that was synthesized possesses a substantial mesoporous surface area and carbon active sites that are devoid of functionalization, which may serve to govern the initial high removal percentage rate. Nevertheless, upon the attainment of equilibrium, the active sites became entirely enveloped by the metal compound, thereby intensifying conflict between the Pb molecules within their own particular environment and consequently impeding the adsorption process. Figure 3 elucidates the fact that elevating the initial concentration will lead to a concomitant enhancement in the adsorption capacity ( $q_e$ ) at equilibrium, provided that the concentration is elevated. In Figure 3, for instance, the equilibrium adsorption capacity increases from 50 mg/g to 660 mg/g when the starting concentration of Pb is increased from 100 mg/g to 1000 mg/g. An increase in the number of collisions between Pb molecules and CFH, a larger mass transfer driving force, or the saturation of all accessible active sites for adsorption at higher metal concentrations could all be contributing factors to the occurrence of a spike in equilibrium adsorption capacity.

### Kinetics studies

The examination of the adsorption kinetics holds paramount importance in ascertaining the rate and establishing the temporal duration necessary to attain a state of equilibrium. This evaluation is predicated upon the examination of the chemical and physical attributes exhibited by both the adsorbent and the adsorbate. The kinetic study employed the same methodologies as previously stated in the batch adsorption experiments. In this investigation, the sample's Pb concentrations were established by taking readings from the solution at time

periods that were previously determined. Two models, the pseudo-first-order and pseudo-second-order models, were used to model the kinetic data and find the rate-governing steps in the adsorption process.

The formulation of the pseudo-first-order model is mathematically expressed by the subsequent formula:

$$q_t = q_e(1 - \exp^{-k_1 t}) \quad (10)$$

In this equation, the rate constant is denoted by  $K_1$ . And  $t$  represents the duration of contact time is expressed by  $t$ , measured in hour.

The present model can be effectively conveyed through the use of the subsequent linearized format:

$$\log(q_e - q_t) = \log(q_e) - \frac{k_1 t}{2.303} \quad (11)$$

The variables  $q_e$  represent the equilibrium adsorption capacity of Pb onto CFH, measured in mg/g. The variable  $q_t$  represents the amount of Pb adsorbed at any given time  $t$  (expressed in minutes), also measured in mg/g. Lastly, the adsorption rate is expressed by  $k_1$ .

The mathematical representation denoting the pseudo-second order kinetic model can be expressed as follows:

$$q_t = \frac{q_e^2 k_2 t}{1 + q_e k_2 t} \quad (12)$$

The preceding model can be expressed in linear format as follows:

$$\frac{t}{q_t} = \left( \frac{1}{k_2 q_e^2} \right) + \left( \frac{1}{q_e} \right) t \quad (13)$$

Here,  $q_e$  (mg/g) denotes the quantity of Pb adsorption on CFH at equilibrium. Alongside, the rate constant is expressed as  $K_2$ .

During the initial time point ( $t = 0$ ), the rate of initial sorption, which is denoted by the symbol  $h$  (mg/g min), can be described in the following manner:

$$h = k_2 q_e^2 \quad (14)$$

The optimal model was selected based on the  $R^2$  values and the average relative error (ARE). Here are specified the formulas utilized for the functions:

$$R^2 = 1 - \frac{\sum_{N=1}^N (q_{e,exp,N} - q_{e,mod,N})^2}{\sum_{N=1}^N (q_{e,exp,N} + q_{e,mod,N})^2} \quad (15)$$

$$ARE = \frac{100}{n} \sum_{i=1}^n \left( \frac{q_{t,exp} - q_{t,mod}}{q_{t,exp}} \right) \quad (16)$$

The variable  $q_{t,exp}$  (mg/g) denotes the empirical adsorption capacity of Pb at a specific time  $t$ , while the anticipated adsorption capacity is denoted by  $q_{t,mod}$  (mg/g). The quantity of observations is denoted by the symbol  $n$ .

The identification of a more suitable model was ascertained considering the elevated magnitude of the  $R^2$  and the diminished values of the ARE. Figure 4 illustrates that the process of Pb adsorption occurred in a biphasic manner at a temperature of 30 °C. During the subsequent phase, the rate of adsorption of Pb exhibited a gradual decline until it ultimately attained a state of equilibrium.

Figure 4 shows that Pb adsorption on CFH may take longer than 8 h to reach equilibrium. This study demonstrated that early reaction phase Pb adsorption from suspension onto hydrochars increased considerably. This is because binding sites were abundant at that time (Ghaedi et al., 2011).

The  $R^2$  value pertaining to the relationship between Pb ions and the kinetic parameters are showcased in Table 6. The data unambiguously demonstrate that the coefficients for alternative kinetic models are larger and closer to 1 for the pseudo-second order. As a result, the high  $R^2$  value (0.999) indicates that the Pb adsorption process on CFHs is consistent with the ideas of pseudo-second-order kinetics. The above findings suggest that chemical sorption dominates the process rate. According to this concept, the adsorption rate is solely controlled by chemical sorption, which occurs when the adsorbate and CFH share electrons

(Ho & McKay, 1999). Nhambe et al. (2024) also found similar result with hydrochar prepared from pulp and paper sludge.

At varying initial concentrations, Table 7 displays the intra-particle diffusion characteristics for Pb adsorption on soil-CFH mixers. The  $R^2$  values associated with the intra-particle diffusion model exhibited superior performance compared to the  $R^2$  values obtained from the film diffusion model across all the investigated initial concentrations. The significant  $R^2$  value and the presence of a non-zero C value indicate that the process of Pb adsorption on CFH is mostly governed by intra-particle diffusion that serves as the deciding factor in determining the rate of the process. Ultimately, the mechanism of Pb adsorption by CFH and soil-CFH mixers can be elucidated by the pseudo-second order kinetics, with intra particle diffusion serving a crucial part in regulating the rate.

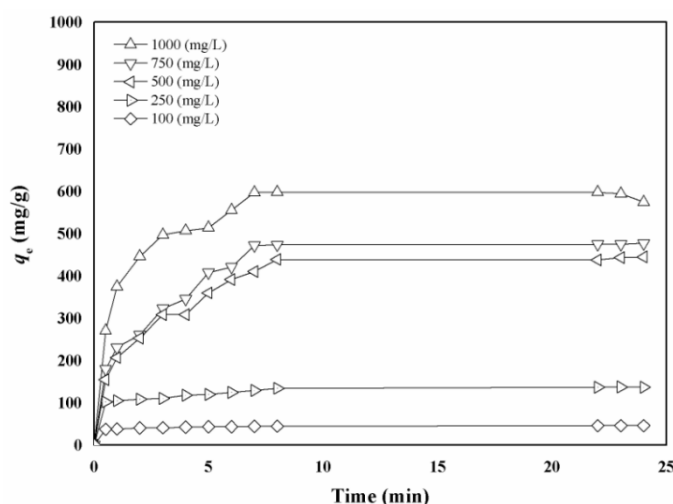


Figure 3: Effect of contact time and initial concentration on the uptake of Pb onto CFH at 30 °C

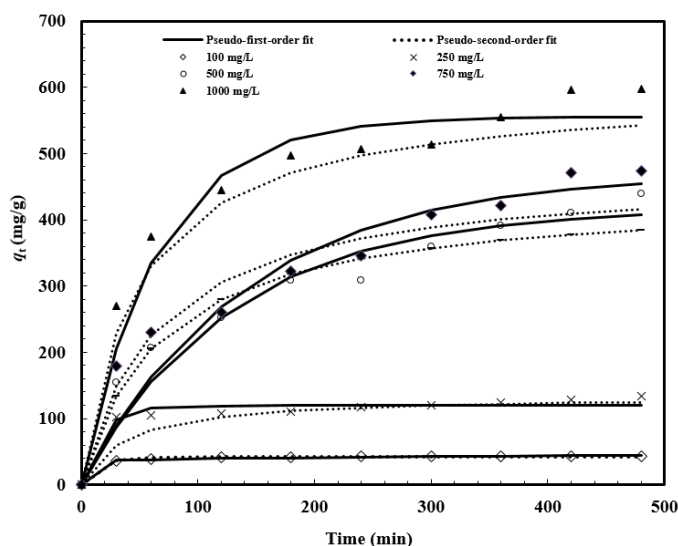


Figure 4: Non-linear plots of Pseudo- first-order and Pseudo- second-order plot for Pb onto CFH at 30 °C



Table 6: Kinetic parameters for the adsorption of Pb onto CFH at different initial concentrations

Parameters	C <sub>0</sub> (mg/L)				
	100	250	500	750	1000
<i>q<sub>e, exp</sub></i> (mg/g)	44.38	134.04	438.75	473.2	597.5
<b>Pseudo-first-order</b>					
<i>q<sub>e, mod</sub></i> (mg/g)	42.13	119.35	417.46	471.02	555.49
<i>k<sub>1</sub></i> (1/m)	0.064	0.057	0.007	0.007	0.015
<i>R</i> <sup>2</sup>	0.456	0.321	0.875	0.878	0.808
ARE	0.025	0.461	7.37	8.32	3.47
<b>Pseudo-Second-order</b>					
<i>q<sub>e, mod</sub></i> (mg/g)	43.62	134.45	438.72	473.20	597.45
<i>k<sub>2</sub></i> (g/mg min)	0.003	0.001	0.001	0.001	0.001
<i>R</i> <sup>2</sup>	0.797	0.990	0.865	0.820	0.999
ARE	0.008	0.104	5.34	6.75	3.25

Table 7: Intraparticle diffusion and Film diffusion parameters at 30 °C

C <sub>0</sub> (mg/L)	Intraparticle diffusion		Film diffusion	
	<i>K<sub>id</sub></i>	<i>R</i> <sup>2</sup>	<i>K<sub>fd</sub></i>	<i>R</i> <sup>2</sup>
100	18.18	0.904	0.001	0.034
250	18.50	0.986	0.005	0.077
500	16.73	0.989	0.002	0.158
750	1.90	0.951	0.005	0.205
1000	0.459	0.983	0.005	0.166

## Conclusion

The adsorption results suggested how the CFH material exhibits considerable potential as an adsorbent due to its substantial active surface area, particularly in the context of removing Pb. A multitude of validated and widely recognized numerical models and configurations were employed in order to juxtapose the empirical observations. The Langmuir model provided a more accurate match to the adsorption isotherm compared to the Freundlich model, as evidenced by the higher *R*<sup>2</sup> value. At a temperature of 40 °C, the highest adsorption capacity (*q<sub>m</sub>*) of CFH was found to be 1426 mg/g. The adsorption capacity rose when the solution pH changed from 2 to 4, reaching its highest level of 233 mg/g. Following the elevation of the pH level from 4, there was a subsequent decline in the adsorption capacity, ranging from 6 to 12. The result is justified by the interaction of *pH<sub>pzc</sub>* and electrostatic force. Hydrochar application on soil with a slightly acidic pH can enhance the adsorption of Pb, therefore aiding in the remediation of the environment. The Pb adsorption data were corroborated by the pseudo-second-order kinetics model. Based on the results of the thermodynamic analysis, it was determined that the method of Pb adsorption was endothermic, spontaneous, and feasible. However, this study has certain limitations, including the lack of characterization of CFH's surface functional groups, surface area, and porosity properties. In conclusion, the CFH synthesized in this investigation exhibits the latent capacity to serve as an advanced and economically efficient adsorbent in the context of environmental pollution mitigation, with a particular emphasis on addressing the issue of Pb contamination.

## Funding Statement

This research was supported by the Khulna University Research cell (Ref: KU/Research cell-04/2000).

## Acknowledgement

We want to express our deepest gratitude to everyone who made important contributions that helped us finish this study project successfully. We are grateful to the Forestry and Wood Technology Discipline and the Environmental Science Discipline for letting us do the study and helping with the logistics. Funding for this study came from the Khulna University Research cell (Ref: KU/Research cell-04/2000).

## Competing Interest

The authors report that there are no competing interests to declare.

## Credit Author Statement

Imran Chowdhury Sakib: Methodology, Laboratory Experiments, Data Analysis, Writing – the first and final draft; Md. Azharul Islam: Co-supervision, Data Analysis, Writing – final draft, review and editing; Rashedul Islam: Methodology, Laboratory Experiments, Writing – methodology and conclusion; Jeba Rezwana: Methodology, Laboratory Experiments, Writing – methodology and conclusion; Md. Atikul Islam: Supervision, Conceptualization, Writing – final draft, review and editing.

## References

- Akter, N., Chakma, S., Fatema, K., Azad, A. K., Jaman Chowdhury, M., & Abu Sayid Mia, M. (2019). Alkali enzymatic extraction of keratin protein from chicken feather waste in Bangladesh. *Iranian (Iranica) Journal of Energy & Environment*, 10(4), 235-241.
- Ali, I. H., Al Mesfer, M. K., Khan, M. I., Danish, M., & Alghamdi, M. M. (2019). Exploring Adsorption Process of Lead (II) and Chromium (VI) Ions from Aqueous Solutions on Acid Activated Carbon Prepared from Juniperus procera Leaves. *Processes*, 7(4), Article 4.
- Archer, A., & Barratt, R. (1976). Lead levels in Birmingham dust. *Science of the total environment*, 6(3), 275-286.
- Assi, M. A., Hezme, M. N. M., Haron, A. W., Sabri, M. Y. M., & Rajion, M. A. (2016). The detrimental effects of lead on human and animal health. *Veterinary World*, 9(6), 660-671.
- Begum, K., Mohiuddin, K., Zakir, H., Rahman, M. M., & Hasan, M. N. (2014). Heavy metal pollution and major nutrient elements assessment in the soils of Bogra city in Bangladesh. *Canadian Chemical Transactions*, 2(3), 316-326.
- Cannon, H. L., & Bowles, J. M. (1962). Contamination of vegetation by tetraethyl lead. *Science*, 137(3532), 765-766.
- Chakraborty, R., Asthana, A., Singh, A. K., Jain, B., & Susan, A. B. H. (2022). Adsorption of heavy metal ions by various low-cost adsorbents: a review. *International Journal of Environmental Analytical Chemistry*, 102(2), 342-379.
- Chakraborty, R., Asthana, A., Singh, A. K., Verma, R., Sankarasubramanian, S., Yadav, S., Carabineiro, S. A., & Susan, M. A. B. H. (2022). Chicken feathers derived materials for the removal of chromium from aqueous solutions: kinetics, isotherms, thermodynamics and regeneration studies. *Journal of Dispersion Science and Technology*, 43(3), 446-460.
- Day, J., Hart, M., & Robinson, M. (1975). Lead in urban street dust. *Nature*, 253(5490), 343-345.
- Debnath, B., Singh, W. S., & Manna, K. (2019). Sources and toxicological effects of lead on human health. *Indian Journal of Medical Specialities*, 10(2), 66-71.
- Earl, R., Burns, N., Nettelbeck, T., & Baghurst, P. (2016). Low-level environmental lead exposure still negatively associated with children's cognitive abilities. *Australian Journal of Psychology*, 68(2), 98-106.
- Faust, S., & Aly, O. (1987). Biological activated carbon treatment of drinking water. *Adsorption process for water treatment*. Butterworth Publishers, Stoneham, Mass, 433-470.
- Flora, G., Gupta, D., & Tiwari, A. (2012). Toxicity of lead: A review with recent updates. *Interdisciplinary Toxicology*, 5(2), 47-58.
- Ge, Q., Tian, Q., Wang, S., Zhang, J., & Hou, R. (2022). Highly Efficient Removal of Lead/Cadmium by Phosphoric Acid-Modified Hydrochar Prepared from Fresh Banana Peels: Adsorption Mechanisms and Environmental Application. *Langmuir*, 38(49), 15394-15403.
- Ghaedi, M., Hassanzadeh, A., & Kokhdan, S. N. (2011). Multiwalled Carbon Nanotubes as Adsorbents for the Kinetic and Equilibrium Study of the Removal of Alizarin Red S and Morin. *Journal of Chemical & Engineering Data*, 56(5), 2511-2520.
- Gilani, S. R., Batool, M., Ali Zaidi, S. R., Mahmood, Z., Bhatti, A. A., & Durrani, A. I. (2015). Central nervous system (CNS) toxicity caused by metal poisoning: Brain as a target organ. *Pakistan Journal of Pharmaceutical Sciences*, 28(4).
- Goodlad, J. K., Marcus, D. K., & Fulton, J. J. (2013). Lead and attention-deficit/hyperactivity disorder (ADHD) symptoms: a meta-analysis. *Clinical psychology review*, 33(3), 417-425.
- Gorini, F., Muratori, F., & Morales, M. A. (2014). The role of heavy metal pollution in neurobehavioral disorders: a focus on autism. *Review Journal of Autism and Developmental Disorders*, 1(4), 354-372.
- Graziotin, A., Pimentel, F., De Jong, E., & Brandelli, A. (2006). Nutritional improvement of feather protein by treatment with microbial keratinase. *Animal feed science and technology*, 126(1-2), 135-144.
- Guilarte, T. R., Opler, M., & Pletnikov, M. (2012). Is lead exposure in early life an environmental risk factor for Schizophrenia? *Neurobiological connections and testable hypotheses*. *Neurotoxicology*, 33(3), 560-574.
- Hammud, H. H., Karnati, R. K., Al Shafee, M., Fawaz, Y., & Holail, H. (2021). Activated hydrochar from palm leaves as efficient lead adsorbent. *Chemical Engineering Communications*, 208(2), 197-209.
- Ho, Y.-S., & McKay, G. (1999). Pseudo-second order model for sorption processes. *Process Biochemistry*, 34(5), 451-465.
- Hu, X., Dai, L., Ma, Q., Xu, J., & Ma, J. (2022). One-pot synthesis of iron oxides decorated bamboo hydrochar for lead and copper flash removal. *Industrial Crops and Products*, 187, 115396.
- Islam, M., Limon, M., Hasan, S., & Romić, M. (2021). Hydrochar-based soil amendments for agriculture: a review of recent progress. *Arabian Journal of Geosciences*, 14(2), 1-16.
- Islam, M. S., Ahmed, M. K., Habibullah-Al-Mamun, M., & Raknuzzaman, M. (2015). The concentration, source and potential human health risk of heavy metals in the commonly consumed foods in Bangladesh. *Ecotoxicology and environmental safety*, 122, 462-469.
- Kambo, H. S., & Dutta, A. (2015). A comparative review of biochar and hydrochar in terms of production, physico-chemical properties and applications. *Renewable and Sustainable Energy Reviews*, 45, 359-378.
- Kennedy, D., Woodland, C., & Koren, G. (2012). Lead exposure, gestational hypertension and pre-eclampsia: a systematic review of cause and effect. *Journal of Obstetrics and Gynaecology*, 32(6), 512-517.
- Koprivica, M., Simić, M., Petrović, J., Ercegović, M., & Dimitrijević, J. (2023). Evaluation of Adsorption Efficiency on Pb(II) Ions Removal Using Alkali-Modified Hydrochar from Paulownia Leaves. *Processes*, 11(5), 1327.

- Langmuir, I. (1918). The adsorption of gases on plane surfaces of glass, mica and platinum. *Journal of the American Chemical society*, 40(9), 1361-1403.
- Li, B., Guo, J.-Z., Liu, J.-L., Fang, L., Lv, J.-Q., & Lv, K. (2020). Removal of aqueous-phase lead ions by dithiocarbamate-modified hydrochar. *Science of the total environment*, 714, 136897.
- Madduri, S., & Elsayed, I. (2020). Novel oxone treated hydrochar for the removal of Pb (II) and methylene blue (MB) dye from aqueous solutions. *Chemosphere*, 260, 127683.
- Malool, M. E., Keshavarz Moraveji, M., & Shayegan, J. (2021). Optimized production, Pb (II) adsorption and characterization of alkali modified hydrochar from sugarcane bagasse. *Scientific Reports*, 11(1), 22328.
- Markus, J., & McBratney, A. B. (2001). A review of the contamination of soil with lead: II. Spatial distribution and risk assessment of soil lead. *Environment international*, 27(5), 399-411.
- Mau, V., Quance, J., Posmanik, R., & Gross, A. (2016). Phases' characteristics of poultry litter hydrothermal carbonization under a range of process parameters. *Bioresource technology*, 219, 632-642.
- Mihajlović, M., Petrović, J., Stojanović, M., Milojković, J., Lopičić, Z., Koprivica, M., & Lačnjevac, Č. (2016). Hydrochars, perspective adsorbents of heavy metals: a review of the current state of studies. *Zaštita materijala*, 57(3), 488-495.
- Motto, H. L., Daines, R. H., Chilko, D. M., & Motto, C. K. (1970). Lead in soils and plants: its relation to traffic volume and proximity to highways. *Environmental science & technology*, 4(3), 231-237.
- Navas-Acien, A., Guallar, E., Silbergeld, E. K., & Rothenberg, S. J. (2007). Lead exposure and cardiovascular disease—a systematic review. *Environmental health perspectives*, 115(3), 472-482.
- Nevin, R. (2000). How lead exposure relates to temporal changes in IQ, violent crime, and unwed pregnancy. *Environmental research*, 83(1), 1-22.
- Nhambe, P., Patel, B., Leswif, T. Y., Abdulsalam, J., & Gardee, N. (2024). Adsorption of lead (II) in a single and multi-metal system by hydrochar from pulp and paper sludge. *International Journal of Environmental Science and Technology*.
- Nigg, J. T., Knottnerus, G. M., Martel, M. M., Nikolas, M., Cavanagh, K., Karmaus, W., & Rappley, M. D. (2008). Low blood lead levels associated with clinically diagnosed attention-deficit/hyperactivity disorder and mediated by weak cognitive control. *Biological psychiatry*, 63(3), 325-331.
- Nzediegwu, C., Naeth, M. A., & Chang, S. X. (2021). Lead (II) adsorption on microwave-pyrolyzed biochars and hydrochars depends on feedstock type and production temperature. *Journal of hazardous materials*, 412, 125255.
- Qishlaqi, A., Moore, F., & Forghani, G. (2008). Impact of untreated wastewater irrigation on soils and crops in Shiraz suburban area, SW Iran. *Environmental Monitoring and Assessment*, 141(1), 257-273.
- Rosignol, D. A., Genuis, S. J., & Frye, R. E. (2014). Environmental toxicants and autism spectrum disorders: a systematic review. *Translational psychiatry*, 4(2), e360-e360.
- Salman, J. M., Njoku, V. O., & Hameed, B. H. (2011). Adsorption of pesticides from aqueous solution onto banana stalk activated carbon. *Chemical Engineering Journal*, 174(1), 41-48.
- Sanders, T., Liu, Y., Buchner, V., & Tchounwou, P. B. (2009). Neurotoxic effects and biomarkers of lead exposure: a review. *Reviews on environmental health*, 24(1), 15-46.
- Santurtún, A., Villar, A., Delgado-Alvarado, M., & Riancho, J. (2016). Trends in motor neuron disease: association with latitude and air lead levels in Spain. *Neurological Sciences*, 37(8), 1271-1275.
- Schroeder, H. A. (1965). Cadmium as a factor in hypertension. *Journal of Chronic Diseases*, 18(7), 647-656.
- Thamer, B. M., Aldalbahi, A., Moydeen A, M., Al-Enizi, A. M., El-Hamshary, H., & El-Newehy, M. H. (2019). Fabrication of functionalized electrospun carbon nanofibers for enhancing lead-ion adsorption from aqueous solutions. *Scientific Reports*, 9(1), 19467.
- Wang, T., Zhai, Y., Zhu, Y., Li, C., & Zeng, G. (2018). A review of the hydrothermal carbonization of biomass waste for hydrochar formation: Process conditions, fundamentals, and physicochemical properties. *Renewable and Sustainable Energy Reviews*, 90, 223-247.
- Wrześniewska-Tosik, K., & Adamiec, J. (2007). Biocomposites with a content of keratin from chicken feathers. *Fibres & Textiles in Eastern Europe*, 15(1), 60.
- Wu, W.-T., Lin, Y.-J., Liou, S.-H., Yang, C.-Y., Cheng, K.-F., Tsai, P.-J., & Wu, T.-N. (2012). Brain cancer associated with environmental lead exposure: Evidence from implementation of a National Petrol-Lead Phase-Out Program (PLPOP) in Taiwan between 1979 and 2007. *Environment international*, 40, 97-101.
- Xia, Y., Yang, T., Zhu, N., Li, D., Chen, Z., Lang, Q., Liu, Z., & Jiao, W. (2019). Enhanced adsorption of Pb (II) onto modified hydrochar: Modeling and mechanism analysis. *Bioresource technology*, 288, 121593.
- Xu, Q., Qian, Q., Quek, A., Ai, N., Zeng, G., & Wang, J. (2013). Hydrothermal carbonization of macroalgae and the effects of experimental parameters on the properties of hydrochars. *ACS Sustainable Chemistry & Engineering*, 1(9), 1092-1101.
- Xue, Y., Gao, B., Yao, Y., Inyang, M., Zhang, M., Zimmerman, A. R., & Ro, K. S. (2012). Hydrogen peroxide modification enhances the ability of biochar (hydrochar) produced from hydrothermal carbonization of peanut hull to remove aqueous heavy metals: batch and column tests. *Chemical Engineering Journal*, 200, 673-680.